Electronic Supplementary Information

An electrochemical biosensor equipped with a logic circuit as a smart automaton for two-miRNA pattern detection

Benting Xie, Shimao Du, Hejun Gao, Juan Zhang*, Hongquan Fu* and Yunwen Liao

College of Chemistry and Chemical Engineering, Chemical Synthesis and Pollution Control Key Laboratory of Sichuan Province, China West Normal University, Nanchong, Sichuan 637000, China

*Corresponding Author:

E-mail: zhangbestone@163.com. (J. Zhang); fubestone@163.com. (F. Q. Fu)

Materials and Reagents. All oligonucleotides, TE buffer (1×, low EDTA, PH 8.0), 5×TBE buffer (250 mM Tris, 10 mM EDTA, 250 mM H_3BO_3, pH 8.0), and agarose (conventional) were purchased by Sangon Biotech Co., Ltd. (Shanghai, China), and the corresponding oligonucleotide sequences were listed in Table S1. Chloroauric acid ($HAuCl_4 \cdot 3H_2O$, AR), magnesium chloride ($MgCl_2$, AR), potassium chloride (KCl, AR), hexamercaptan (HT, 96%), disodium hydrogen phosphate (Na_2HPO_4, AR), potassium dihydrogen phosphate (KH_2PO_4, AR), potassium ferricyanide ($K_3[Fe(CN)_6$, AR), potassium ferrocyanide ($K_4[Fe(CN)_6$, AR). Alumina polishing powder was purchased from Tianjin Aida Hengsheng Technology Development Co., Ltd. (Tianjin, China). A 5.0 mM $[Fe(CN)_6]^{3-/4-}$ solution (5.0 mM $K_3[Fe(CN)_6]$, 5.0 mM $K_4[Fe(CN)_6]$, 0.1 M KCl, pH 7.4) was used as the supporting electrolyte for cyclic voltammetry (CV) and electrochemical impedance spectroscopy (EIS) detection. Prepare square wave voltammetry (SWV) detection buffer with PBS. The aqueous solution was prepared from ultrapure water (Shanghai Hetai Instrument Co., Ltd.) obtained by the Hitech-Sciencetool water purification system. Oligonucleotide sequences were synthesized by Sangon Biotech Co., Ltd. (Shanghai, China), and the sequences were listed in Table S1.

Apparatus. In this work, all electrochemical measurements were performed at the CHI 660E electrochemical workstation (Shanghai Chenghua Instrument Co., Ltd.) using a conventional three-electrode system, in which the glassy carbon electrode (GCE, Φ = 4 mm) was the working electrode, the Ag/AgCl electrode (saturated KCl) was the reference electrode, and the platinum wire was the auxiliary electrode. The electrodes used in the experiment were purchased from Tianjin Aida Hengsheng Technology Development Co., Ltd. (Tianjin, China). 4% agarose gel electrophoresis results were obtained in JY300E.

Table S1. The sequences are listed below as text sequences annotated with segment names.

Names	Sequence (5′ to 3′)
miR-21	TAGCTTATCAGACTGATGTTGA TAGCTTATCAGACTGATGTTGA(OR, denoted by 1a-1b) TAGCTTATCAGACTGATGTTGA (AND, denoted by 1m-1n)
miR-122	TGGAGTGTGACAATGGTGTTTG TGGAGTGTGACAATGGTGTTTG(OR, denoted by 2a-2b) TG, GAGTGTGACAATGGTGTTTG(AND, denoted by $2m_1$, $2m_2$ -2n)
S	CAAACACCATTGTCACACTCCATCAACATCAGTCTGATAAGCTA TTTTTTTTTT CAAACACCATTGTCACACTCCATCAACATCAGTCTGATAAGCTA TTTTTTTTTT (OR, denoted by 2b*-2a*-1b*-1a*- T_{10}) CAAACACCATTGTCACA,CTCCATCAACATCAGTCTGATAAGCT A TTTTTTTTTT(AND, denoted by 2n*- $2m_1$, $2m_2$ *-1n*-1m*- T_{10})
S-SH	CAAACACCATTGTCACACTCCATCAACATCAGTCTGATAAGCTA TTTTTTTTTT – SH
F_O	ACTAGTGCGATGTTGATGGAGTGTGCACTAGT(OR, denoted by x-1b-2a-x*)
F_O-Fc	Fc-ACTAGTGCGATGTTGATGGAGTGTGCACTAGT
F_A	TCAGACTGATGTTGATGTGTGACAATGGTGTTTG (AND, denoted by 1n-$2m_1$-2n)
F_A-Fc	Fc-TCAGACTGATGTTGATGTGTGACAATGGTGTTTG
miRNA-155	TTAATGCTAATCGTGATAGGGGT
miRNA-16	TAGCAGCACGTAAATATTGGCG

Preparation of F_O-Fc and F_A-Fc

Firstly, the phosphorite of ferrocene reacted with the hydroxyl group on the F_A or F_O to form a phosphoric acid bond, which coupled to F_A or F_O (Fig. S1). Then, F_O-Fc and F_A-Fc were purified by high performance liquid chromatography (HPLC). As been seen in Fig. S2, the molecular weight (MW) of F_A is 10576.4 μg/μmol (Fig.

S2A). While Fc is labeled the at the 5' end of F_A, the MW of F_A-Fc is 10963.3 μg/μmol (Fig. S2B). The value keeps consistent of the theoretical value (MW_{FA}+ MW_{Fc}=10576.4+390.70=10967.1 μg/μmol), which further proved that F_A-Fc was successfully prepared. Similarly, MW of F_O is 9952.4 μg/μmol (Fig. S3A). After Fc is labeled the at the 5' end of F_O, the MW of F_A-Fc is 10340.8 μg/μmol (Fig. S3B). The value approximately equals to the theoretical value (MW_{Fo}+MW_{Fc}=9952.4+390.70= 10343.1 μg/μmol), suggesting that F_O-Fc was successfully prepared.

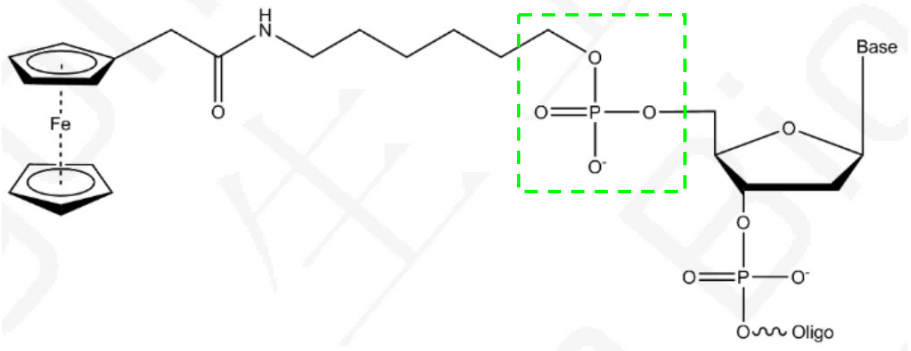

Fig. S1. The principle of Fc-labeled single strand DNA.

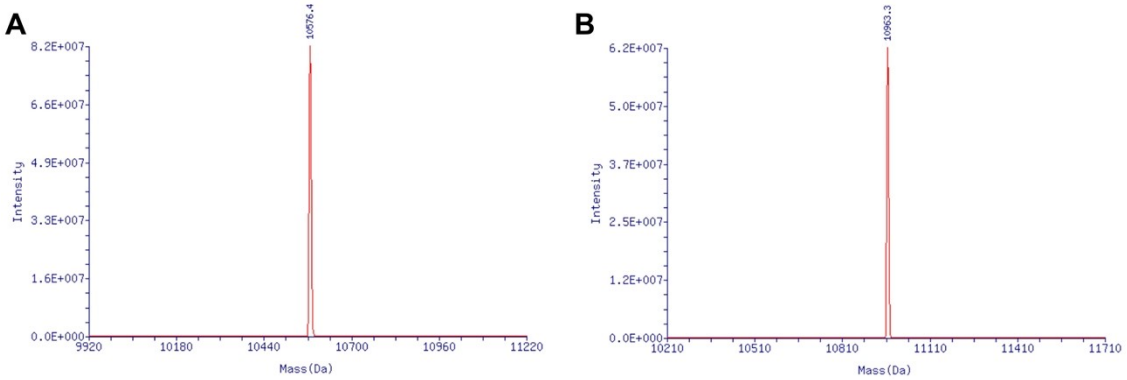

Fig. S2. The mass spectrogram of F_A (A) and F_A-Fc (B).

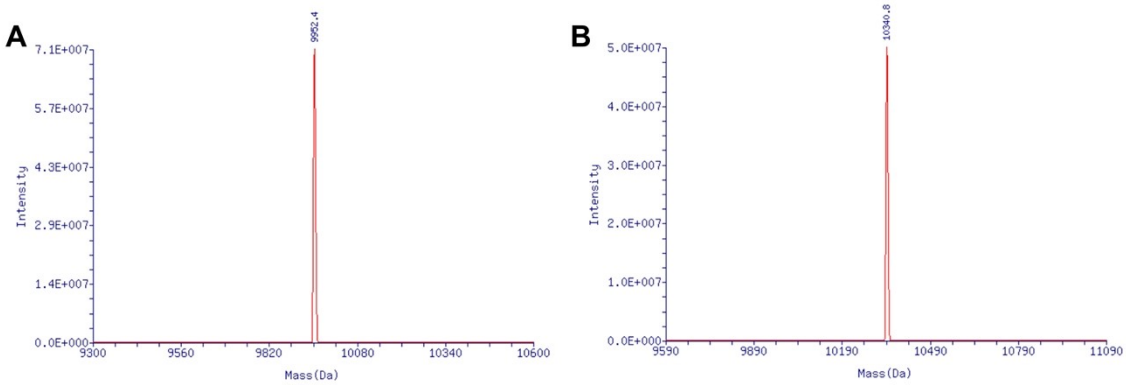

Fig. S3. The mass spectrogram of F_o (A) and F_o-Fc (B).

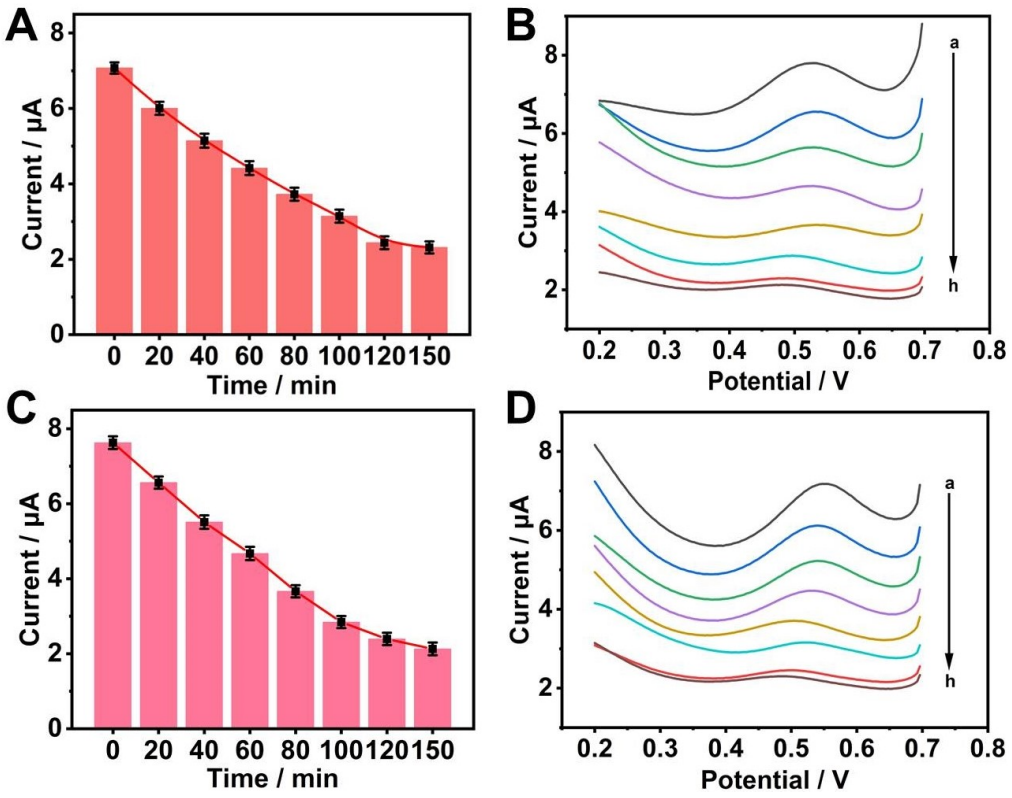

Fig. S4. Optimization of the incubation time of miR-21 and miR-122. The electrochemical signal responses (A) and corresponding SWV curve (B) for AND measuring automata; The electrochemical signal responses (C) and corresponding SWV curve (D) for OR measuring automata.

Calculation of LOD

According to related references and the IUPAC recommendation[1-3], the limit of detection (LOD) was be estimated as LOD = kS_b/m, in which S_b was the standard deviation of the blank signals (n_b = 20), m was the analytical sensitivity which could be estimated as the slope of calibration curve at lower concentration ranges and k is the numerical factor chosen in accordance with the desired confidence level. As suggested by Long and Winefordner[4], the use of k = 3 allows a confidence level of 99.86% for a normal distribution of the blank signals. So, LOD was usually defined as LOD = 3S_b/m. Firstly, to calculate the LOD of the AND measuring automata, the trends of current change values with the concentration of miR-21 and miR-122 was showed. As shown in Fig. S2A, the insert presented that current change value (ΔI) was linearly related to the concentration of miR-21 and miR-122 (c / fM) at a low concentration range. The corresponding linear equation was ΔI = 0.1314 c + 0.2773 and the S_b of twenty times zero-dose was about 0.1669. Therefore, the LOD of the proposed AND measuring biosensor were 3.81 fM (LOD = 3 × 0.1669 ÷ 0.1314 = 3.81 fM). In addition, we also calculated the LOD of the OR measuring automata using the same method. As seen in Fig. S5B, the oxidation peak current change values (ΔI) of Fc increased with the increasing concentration of miRNA-21. The insert presented that ΔI was linearly related to the concentration of miR-21 and miR-122 (c / fM) at a low concentration range. The corresponding linear equation was ΔI = 0.0913 c + 0.2667 and the S_b of twenty times zero-dose was about 0.1470. Therefore, the LOD of the OR measuring biosensor were 4.83 fM (LOD = 3 × 0.1470 ÷ 0.0913 = 4.83 fM).

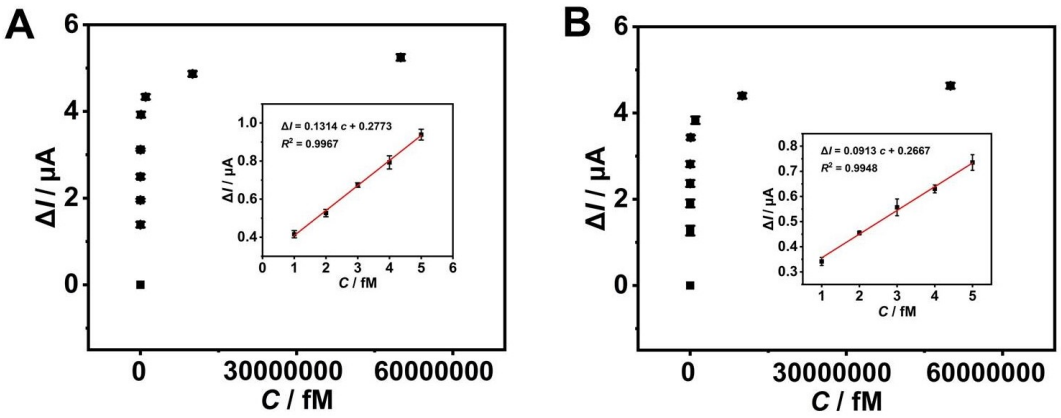

Fig. S5. (A) The variation trend of AND measuring automata responses with miR-21 and miR-122 concentration. The inset shows the calibration curve of current change responses changing with the target in the lower concentration range. (B) The variation trend of AND measuring automata responses with miR-21 and miR-122 concentration. The inset shows the calibration curve of current change responses changing with the target in the lower concentration range.

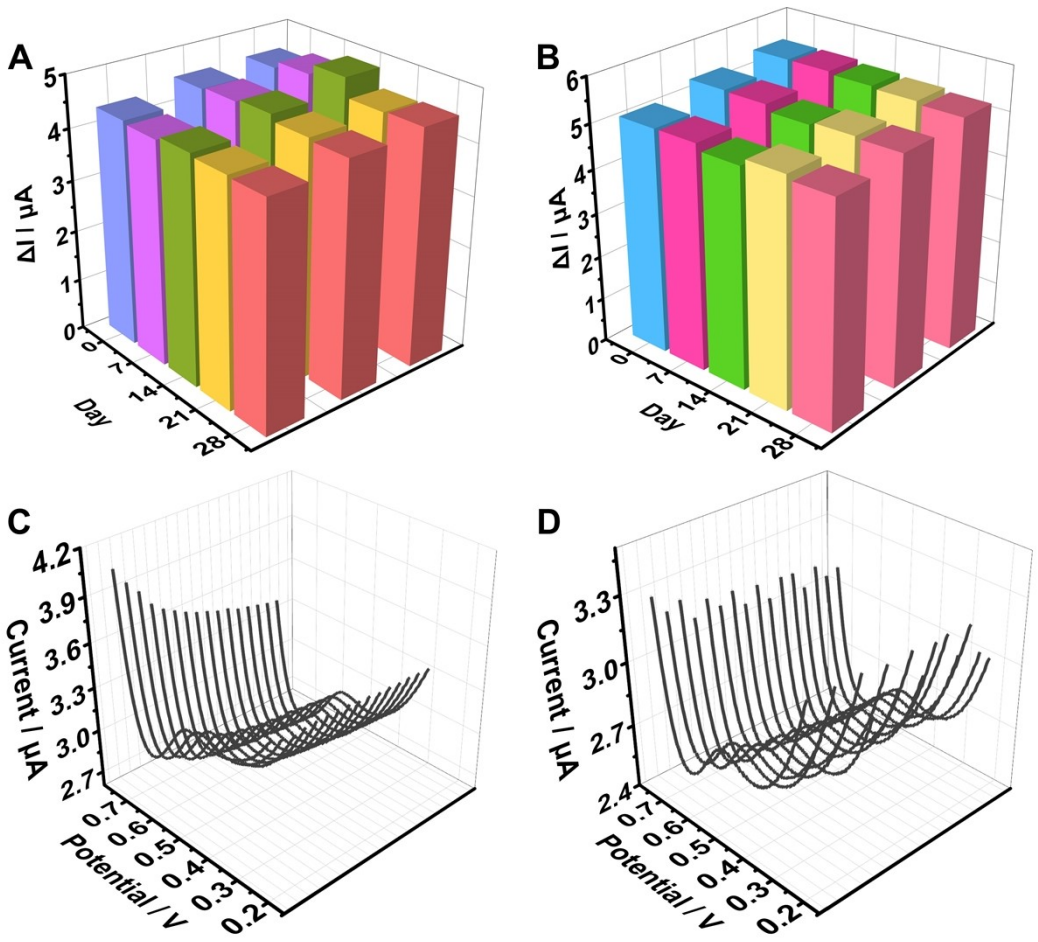

Fig. S6. The store stability of the as-prepared AND (A) and OR (B) measuring electrochemical biosensor (miR-21 and miR-122 at 1 nM). The stability of the as-prepared AND (C) and OR (D) measuring electrochemical biosensor (miR-21 and miR-122 at 1 nM) under 16 repetitive cyclic scans.

Table S2. Comparison of different methods for miR-21 and miR-122 detection

Target	Detection methods	Detection limit	Detection range	ref
miR-21 / miR-20a / miR-106a	SWV	10^{-17} M / Not calculated/Not calculated	10^{-16} to 10^{-13} M	5
miR-21	SWV	2.6×10^{-13} M	10^{-12} to 10^{-8} M	6
miR-21 / APE1	Fluorescence	22.9 pM/12.3 pM	0 to 200 nM	7
miR-21	QCM	3.6 pM	2.5 pM to 2.5 uM	8
miR-21	ECL	8.19 fM	0.01 pM to 1000 pM	9
miR-21	SWV	0.0003 nM	0.001 to 10 nM	10
miR-21 / miR-122	Fluorescence	Not mentioned	0 to 200 nM (OR) / 0 to 500 nM (AND)	11
miR-21 / cells	Fluorescence	0 to 2000 pM / 0 to 1.6×10^{4} cells/uL	34 pM / 100 cells/uL	12
miR-122	Fluorescence	10^{-13} M	0 to 10^{-12} M	13
miR-122	Fluorescence	0.6 pM	4 to 1×10^{5} pM	14
miR-21 / miR-335 / miR-122 / miR-155	Fluorescence	30 pM	0.01 to 1 nM	15
miR-21 / miR-122	Fluorescence	0.48 nM / 0.2 nM	0 to 200 Nm / 0 to 500 nM	16
miR-21 / miR-122	SWV	3.81 fM (AND) / 4.83 fM (OR)	0 to 50 nM	this work

Quantitative Reverse Transcription-PCR (qRT-PCR) Analysis of miR-21 and miR-122. Total 50 μL cellular RNAs were extracted from HepG2, HeLa and HEK 293T cells (~10000) using Trizol reagent (Sangon Co. Ltd., Shanghai, China) according to the manufacturer's instructions. 10 μL of the cDNA samples were prepared by using the reverse transcription (RT) reaction with AMV First Strand cDNA Synthesis Kit (BBI, Toronto, Canada), where 1 μL cellular RNAs was added. The cDNA samples were store at -20 °C for future use. qPCR analysis of cDNA was performed with SybrGreen PCR Master Mix (ABI, USA) on an ABI StepOnePlus qPCR instrument. The 20 μL reaction solution contained 1 μL above cDNA sample diluted 10 times, 10 μL of 2× SybrGreen qPCR Master Mix, 0.4 μL of 10 μM reverse primer, 0.4 μL of 10 μM forward primer and 8.2 μL nuclease-free water. The PCR conditions were as follows: an initial 95 °C for 3 min followed by 35 cycles of 95 °C for 30 s, 57 °C for 30 s , 72 °C for 30 s and 72 °C for 8 min. The primers used in this experiment were: miR-21-3p reverse primer, 5'-CTC AAC TGG TGT CGT GGA GTC GGC AAT TCA GTT GAG ACA GCC CA-3'; miR-21-3p forward primer, 5'-ACA CTC CAG CTG GGC AA CAC CAG TCG A-3'. miR-122-3p reverse primer, 5'-CTC AAC TGG TGT CGT GGA GTC GGC AAT TCA GTT GAG TAT TTA GT-3'; miR-122-3p forward primer, 5'-ACA CTC CAG CTG GGA ACG CCA TTA TCA C-3'.

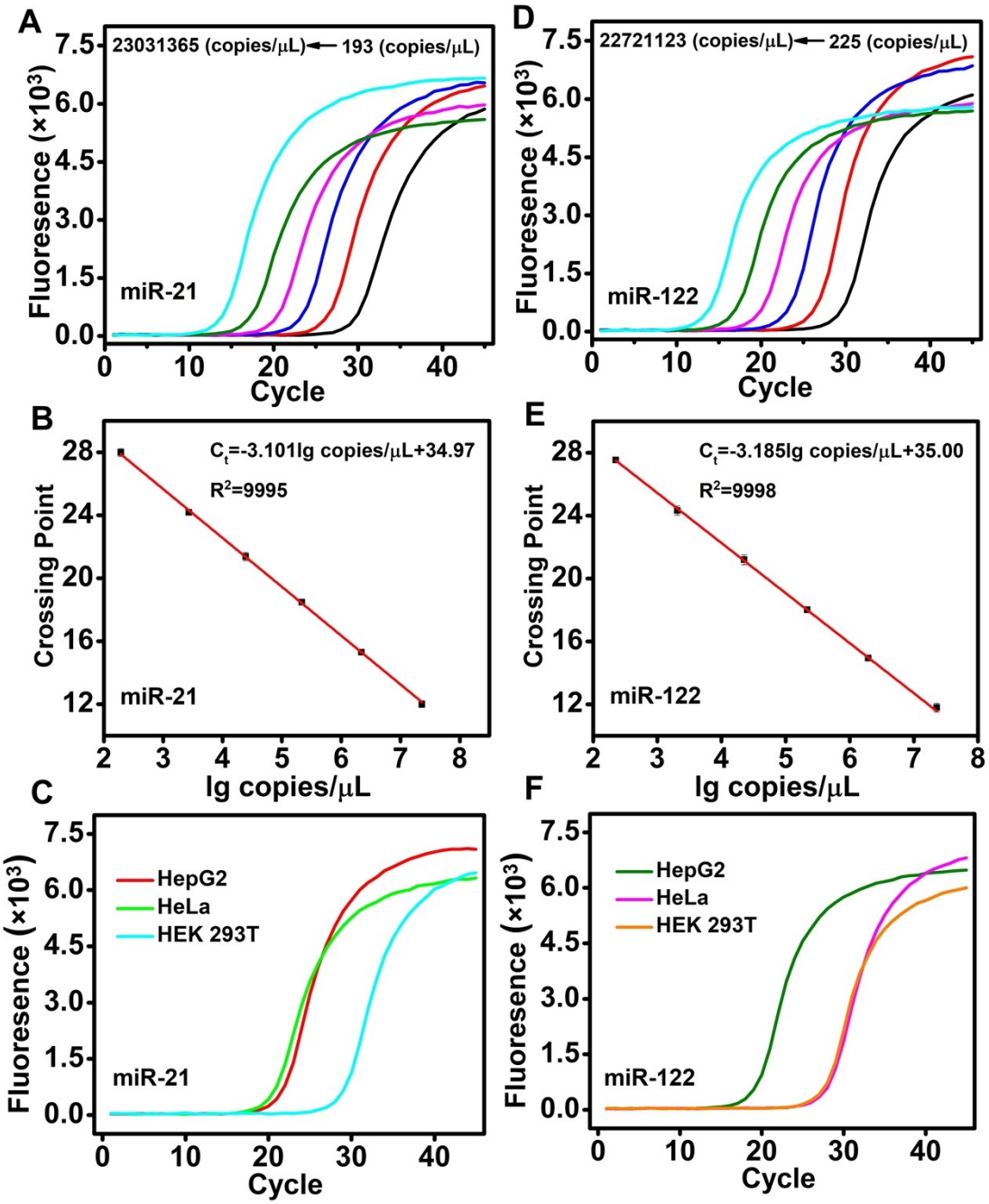

Fig. S7. (A) qRT-PCR amplification plot for miR-21 plasmid. (B) qRT-PCR standard curve for miR-21 plasmid. (C) Quantitative real-time fluorescence detecting of the miR-21 qRT-PCR analysis triggered by tested cell lysates of HepG2, HeLa and HEK 293T. (D) qRT-PCR amplification plot for miR-122 plasmid. (E) qRT-PCR standard curve for miR-122 plasmid. (F) Quantitative real-time fluorescence detecting of the miR-122 qRT-PCR analysis triggered by tested cell lysates of HepG2, HeLa and HEK 293T.

Table S3. Mean concentration of miR-21 in HepG2, HeLa and HEK 293T cell lines

Cell	Mean C_t	Mean copies/μL	Mean *c*/pM
HepG2	19.50067	96922.01	1.61
HeLa	18.32334	219035.40	3.64
HEK 293T	24.00862	1111.903	0.018

Table S4. Mean concentration of miR-122 in HepG2, HeLa and HEK 293T cell lines

Cell	Mean C_t	Mean copies/μL	Mean *c*/pM
HepG2	19.09065	98728.06	1.64
HeLa	24.0807	892.4414	0.015
HEK 293T	24.04197	865.7696	0.014

The absolute expression levels of miR-21 and miR-122 were calculated according to C_t value of data (Fig. S7C and F), the linear calibration curve of data (Fig. S7B and E) and equation:

$$c = \frac{copies/\mu L * 200}{N_A} \times 50$$

N_A is 6.02×10^{23} mol^{-1}; 200 is dilution volume of RNA; 50 is extract volume of RNA.

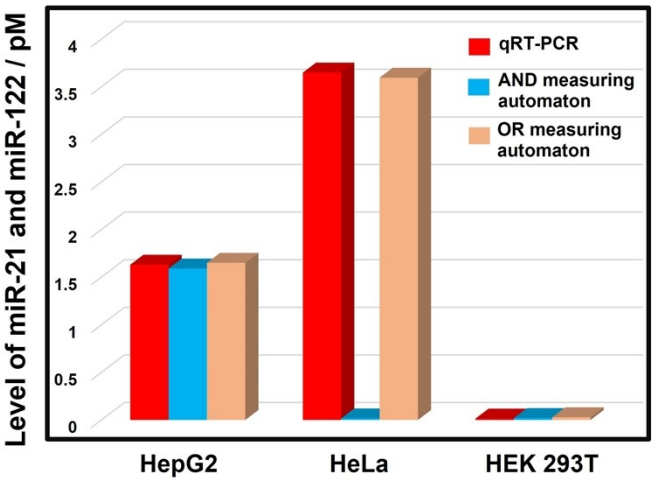

Fig. S8. Real sample analysis of miR-21 and miR-122 detection in different cell lysates (HepG2, HeLa and HEK 293T).

Table S5 Recovery Tests of miR-21 and miR-122 in Human Serum with the Proposed AND measuring automata

Sample	Added (pM)	found (average) (pM)	RSD (%)	rate of recovery (%)
1	1	0.94	3.27	94
2	10	10.76	2.07	107.6
3	100	100.13	1.04	100.1
4	1000	1020.65	1.74	102.1

Table S6 Recovery Tests of miR-21 and miR-122 in Human Serum with the Proposed OR measuring automata

Sample	Added (pM)	found (average) (pM)	RSD (%)	rate of recovery (%)
1	1	1.02	3.71	102
2	10	10.86	3.87	108.6
3	100	92.93	1.88	92.9
4	1000	998.14	2.28	99.8

Reference

1 R. P. Buck and E. Lindner, *Pure Appl. Chem.* 1994, **66**, 2527-2536.

2 L. A. Currie, *Pure Appl. Chem.* 1995, **67**, 1699-1723.

3 A. E. Radi, J. L. Acero Sánchez, E. Baldrich, C. K. O'Sullivan, *J. Am. Chem. Soc.* 2006, **128**, 117-124.

4 G. L. Long and J. D. Winefordner, *Anal. Chem.* 1983, **55**, 712A-724A.

5 P. Miao and Y. G. Tang, *ACS Cent. Sci.*, 2021, **7**, 1036-1044.

6 D. Zhu, W. Liu, D. X. Zhao, Q. Hao, J. Li, J. X. Huang, J. Y. Shi, J. Chao, S. Su and L. H. Wang, *ACS Appl. Mater. Interfaces.*, 2017, **9**, 35597-35603.

7 Z. H. Cai, A. L. Wang, Z. L. Qiu, Y. T. Li, H. R. Yan, M. Y. Fu, M. Y. Liu, Y. Y. Yu and F. L. Gao, *Anal. Chem.*, 2022, **94**, 9715-9723.

8 B. G. Harvey, A. J. Guenthner, T. A. Koontz, P. J. Storch, J. T. Reams and T. J. Groshens, Green Chem., 2016, **18**, 2416-2423.

9 Z. Q. Ning, E. Yang, Y. J. Zheng, M. Y. Chen, G. Q. Wu, Y. J. Zhang and Y. F. Shen, *Anal. Chem.*, 2021, **93**, 8971-8977.

10 W. Q. Bai, A. P. Cui, M. Z. L, X. Z. Q, Y. Li and T. Wang, A*nal. Chem.*, 2019, **91**, 11840-11847.

11 L. Liu, N. Li, Z. M. Huang, L. J. T, Z. M. Y and J. H. Jiang, *Anal. Chem.*, 2020, **92**, 10925-10929.

12 J. Wang, K. X. Wang, H. Y. Peng, Z. Zhang, Z. G. Yang, M. Y. Song and G. B. jiang, *Anal. Chem.*, 2023, **95**, 4138-4146.

13 H. Ren, Z. Long, X. T. Shen, Y. Zhang, J. H. Sun, J. Ouyang and N. Na, *ACS Appl. Mater. Interfaces.*, 2018, **10**, 25621-25628.

14 X. F. Yu, S. Y. Zhang and W. Wang, *Anal. Methods.*, 2022, **14**, 1715-1720.

15 N. N. Wang, L. R. Song, T. Deng and J. S. Li, Analytica Chimica Acta, 2020, **1140**, 69-77.

16 P. Yin, M. M. Ge, S.Y. Xie, L. Zhang, S. K, Z. Nie, Chem. Sci., 2023, **14**, 14131-14139.